

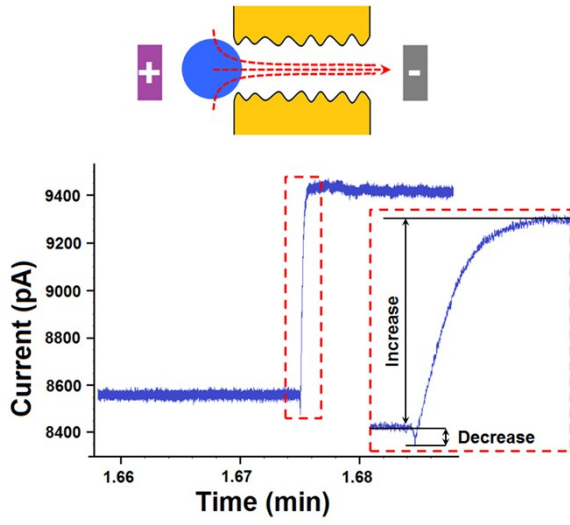
# Probing Charges on Solid-Liquid Interfaces with the Resistive-Pulse Technique

Yinghua Qiu<sup>1</sup> and Zuzanna Siwy<sup>1,2,3</sup>

<sup>1</sup>Department of Physics and Astronomy, <sup>2</sup>Department of Chemistry, <sup>3</sup>Department of Biomedical Engineering, University of California, Irvine, CA 92697

## Abstract

Our manuscript addresses the issue of probing an effective surface charge that any surface can acquire at the solid/liquid interface. Even if a particle is predicted to be neutral based on its chemical structure, the particle can carry finite surface charges when placed in a solution. We present tools to probe the presence of surface charge densities of meso-particles, characterized with zeta potentials below 10 mV. The tools are based on the resistive-pulse technique, which uses single pores to probe properties of individual objects including molecules, particles, and cells. Experiments presented were performed with particles 280 and 400 nm in diameter and single pores with opening diameter tuned between ~ 200 nm and one micron. Surface charge properties were probed in two modes: (i) the passage of the particles through pores of diameters larger than the particles, as well as (ii) an approach curve of a particle to a pore that is smaller than the particle diameter. The curve in the latter mode has a biphasic character starting with a low-amplitude current decrease, followed by a current enhancement reaching an amplitude of ~10% of the baseline current. The current increase was long-lasting and stable, and shown to strongly depend on the particle surface charge density. The results are explained via voltage-modulation of ionic concentrations in the pore.



Surface charge of particles can be probed via an approach curve of individual particles to a pore.

## Introduction

Transport of particles in micropores can occur through several mechanisms. The most common mechanisms include electrophoresis and electroosmosis, transport caused by a pressure difference, and a combination of electrokinetics and the pressure-induced flow.<sup>1</sup>

<sup>2</sup> Electroosmosis is induced in pores whose walls carry excess surface charge.<sup>3</sup> Counterions residing close to the walls follow the direction of the applied field and drag solvent molecules with them, resulting in a net solution flow. In a pore with negative surface charges, electroosmotic flow occurs towards a negatively biased electrode. If the particles are charged, there will also be an electrophoretic force acting on them e.g. electrophoretic force on negatively charged particles will be directed towards a positively biased electrode. With no pressure difference applied, the particles will move in the direction of electrophoresis if their zeta potential is higher than the zeta potential of the pore walls.<sup>4</sup> If the zeta potential of particles is lower than that of the pore walls, the translocation will occur in the direction of electroosmosis i.e. towards a negatively biased electrode.

Neutral particles, such as unmodified polystyrene or PMMA particles, have been used as a probe to understand electroosmotic transport in pores as well as to probe surface charges of the pore walls.<sup>3-8</sup> This is because the translocation speed measured at different transmembrane potentials can be related with the zeta potential of the pore via the Einstein-Smoluchowski equation.<sup>1</sup> In the resistive-pulse technique, a passage of an individual particle is detected as a transient increase of the system resistance, called a pulse, when a particle is in the pore.<sup>2, 9-13</sup> Duration of the pulse is a measure of the particle speed while the distribution of the transit times/velocity can be informative on the

trajectories the particles can follow when in the pore.<sup>7, 12, 14-16</sup> Neutral particles also serve as a model system for understanding transport of exosomes and liposomes as well as for developing tools to detect and isolate them.<sup>2, 17-19</sup> It is important to recognize however that in a real system of a solid-liquid interface, a perfectly neutral surface may not exist. This is because a surface can acquire an excess charge by a variety of different mechanisms including ionic adsorption, surface group deprotonation or dissociation.<sup>20</sup> Consequently, as mentioned above, the particles with finite charges will be moved by a combination of electroosmosis and electrophoresis;<sup>1, 4</sup> in this case, the information on the particle or the pore walls' surface charge cannot be easily probed, because the transit time will be proportional to the difference between pore walls and particles' zeta potential values, not the zeta potential of the pore only.

Here we present experiments of the electrokinetic passage of particles through single polymer micropores, and discuss how the resistive-pulse approach can provide information on the presence of minute amounts of charge. In the classical resistive-pulse set-up, when approaching the pore and when in the pore, a particle blocks the current to an extent, which is determined by the pore and particle dimensions.<sup>2, 9, 10, 13, 21</sup> The pulse duration has already been used to measure zeta potential,  $\zeta$ , of particles with an emphasis on particles characterized by  $\zeta$  of at least 10 mV.<sup>2, 11, 22-24</sup> Here, we discuss other characteristics of resistive-pulses, beyond duration, which are also sensitive to the presence of surface charges, including those resulting in  $\zeta$  only of a few mV. The properties include the magnitude of the pulses corresponding to the beginning and end of the translocations. We have also proposed using pores with a diameter smaller than the particles examined to record an electroosmotic approach curve of individual particles

to the mouth of the pore. The particles' approach was detected as a current increase above the baseline current, even though all pores and particles used in the experiments had diameters exceeding the Debye screening length by hundreds of times. This finding was surprising, because the amplitude of the current increase reached even 10% of the baseline current, thus it was significantly higher than the amplitude of the current decrease in a typical resistive-pulse experiment in which the particles pass through the pore.<sup>6, 17, 25-29</sup> Numerical modeling presented here revealed that the current enhancement was very sensitive to changes in the particles' surface charges. The results are applicable to understanding effective surface charge, however minute, created on the liquid/solid interface.

## **Methods: Experiments and Modeling**

*Preparation of pores:* Single micropores were prepared in 12  $\mu\text{m}$  thick polyethylene terephthalate (PET) films by the track-etching technique.<sup>30</sup> After irradiation with single energetic heavy ions (11.4 MeV/u Au or Bi ions at the Institute for Heavy Ions Research in Darmstadt, Germany)<sup>31</sup> the films were etched in 0.5 M or 2 M NaOH at 70 or 60  $^{\circ}\text{C}$ , respectively. Both etching protocols were found to lead to cylindrical pores whose diameter increased linearly with the etching time.<sup>32</sup> The effective pore size was evaluated using the pore resistance obtained through recording a current-voltage curve in 1 M KCl solution, pH 8.<sup>33</sup> At least three voltage scans were performed, which revealed the current was stable with a standard deviation below 5%. Due to the laminar and semicrystalline structure of PET films we used, the fabricated pores usually have rough inner surfaces,

resulting in fluctuations of the local pore diameter, reaching on average ~15% of the average pore diameter.<sup>34, 35</sup>

*Detecting particles:* Unmodified 280 nm and 400 nm in diameter polystyrene (PS) and 400 nm in diameter poly (methyl methacrylate) (PMMA) particles (Bangs Laboratories, Fisher, IN, USA) were used in the majority of experiments presented here. Some additional measurements were performed with 280, 400 and 410 nm carboxylated polystyrene particles.<sup>36, 37</sup> As reported before, based on dynamic light scattering and resistive-pulse experiments, the standard deviation of the particles' sizes was found not to exceed 10% of the nominal values.<sup>36, 38</sup> Particle suspensions contained  $\sim 10^9$  particles per mL and were prepared based on 0.1 M KCl solution at pH 10 with 0.01% (v/v) Tween 80 or 20. A few experiments performed in 0.05 and 0.3 M KCl are reported as well. Tween 80 was used for preparation of suspensions of PS particles; PMMA suspensions contained Tween 20. As shown in Figure 1a illustrating our experimental set-up, a particle suspension was placed only on one side of the pore; the other side was in contact with a KCl solution without particles. Each chamber of our conductivity cell had a macroscopic volume of  $\sim 1.5$  mL. A pair of Ag/AgCl electrodes was used to apply the voltage and measure the transmembrane current; no pressure difference was applied. The ionic current was monitored with a patch clamp amplifier<sup>39</sup> Axopatch 200B and 1322A Digidata (Molecular Devices, Inc.) under a sampling frequency of 20 kHz. The recorded data were subjected to a low-pass Bessel filter of 1 kHz.

*Numerical modeling:* Coupled Poisson-Nernst-Planck and Navier-Stokes equations were solved with Comsol Multiphysics 4.4 package for single pores with opening diameters of 500 and 260 nm.<sup>6, 16, 36</sup> All solutions provided are steady-state thus no

transient states were considered. The temperature was set as 298 K. The mesh size of 0.2 nm was used for the charged pore surface; for the charged boundary of the reservoirs the mesh of 0.5 nm was chosen. Diffusion coefficient for potassium and chloride ions was assumed equal to the bulk value of  $2 \times 10^{-9} \text{ m}^2/\text{s}$ . All simulations were performed in 100 mM KCl as the bulk electrolyte assuming a relative dielectric constant of water of 80. Surface charge was placed on the pore walls and on the outer membrane surfaces. Figure S1a shows the scheme of a pore that is 500 nm diameter and 2.5  $\mu\text{m}$  in length, used to predict resistive-pulses caused by 200 nm in diameter particles. The modeling was performed for a pore that was 2.5  $\mu\text{m}$  long, not  $\sim 11 \mu\text{m}$  as studied experimentally, due to a very fine mesh (0.05 nm) that was necessary to reach convergence of the system. Note that the pulses were predicted by placing a particle at different axial positions of the pore, thus the particle motion was not modeled directly. Figure 1b presents a scheme of a model used to predict ion current when a particle approached an opening of a pore with diameter smaller than the particle size. The length of this pore was changed between 1  $\mu\text{m}$  and 11  $\mu\text{m}$ . Details of all boundary conditions for both models are shown in Table S1.

## Results and Discussion

### *Electrokinetic passage of particles through single pores.*

Unmodified polystyrene particles were first examined in the resistive-pulse mode, in which they passed through single pores with diameters larger than the particles' diameter. Figure 1b shows example pulses obtained with 280 and 400 nm in diameter polystyrene particles, and a 660 nm in diameter pore. The particle detection was performed from a mixture, and the particles of different sizes were easily recognized by the amplitude of the resistive pulses. The experiments were carried out in a range of voltages between 0.6 V and 1.4 V; example pulses are shown in Figure 2. The average amplitude of the pulses was found to correspond to the particle sizes, as predicted by the resistive-pulse formula relating particle and pore volumes (not shown).<sup>2, 10, 13</sup> The modulations of the current within the pulse are primarily caused by the pore roughness.<sup>34</sup> Note however that the smaller (larger) current decrease in the beginning (end) of the pulse (noted as \* in Figure 2) is not related with the pore topography. **The evidence for this is that when** the particles were placed on the opposite side of the membrane (Figure 2d), and electroosmotically driven by voltage of the opposite voltage polarity, a similar pore asymmetry of the pulses was obtained; the pulses again started with a smaller current decrease, and ended with the largest magnitude of  $\Delta I/I$ . The peaks in the middle of the pulses however are mirror images of each other, indicating the particles in (a-c) and (d) passed in opposite directions.<sup>34</sup> The peaks' asymmetry observed here disappears in higher concentrations of bulk electrolyte (Figure S2), as analyzed in the later part of the manuscript.

The data sets were first analyzed for the pulse duration. Figure 3 compares histograms of passage time of PS particles at 1.4 V through three independently prepared pores of

similar lengths but different opening diameter: 660, 920, and 1290 nm. The average duration time in the full range of examined voltages for the 660 nm pore is summarized in Figure S3. The analysis suggested the electroosmotic velocity was largely independent of the particle or pore size, with the exception of the 660 nm pore, which slowed down the 400 nm beads to a larger extent than the 280 nm spheres.<sup>34, 40</sup> The slightly slower speed of particles in the two wider pores, compared to the 660 nm pore, could result from their increased roughness; it is known that the fluctuations of local diameter increase with the etching time.<sup>41</sup>

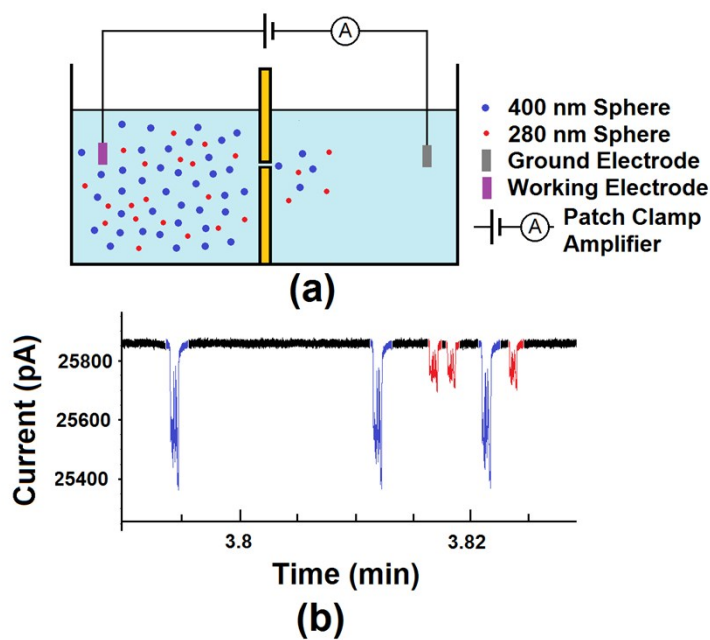


**Figure 1.** (a) *Experimental setup used to detect passage of polystyrene (PS) particles through pores.* (b) *An example of a time series showing individual PS particle passing through a 660 nm PET pore under 0.8 V. Events for 280 and 400 nm particles are shown in red and blue, respectively.*

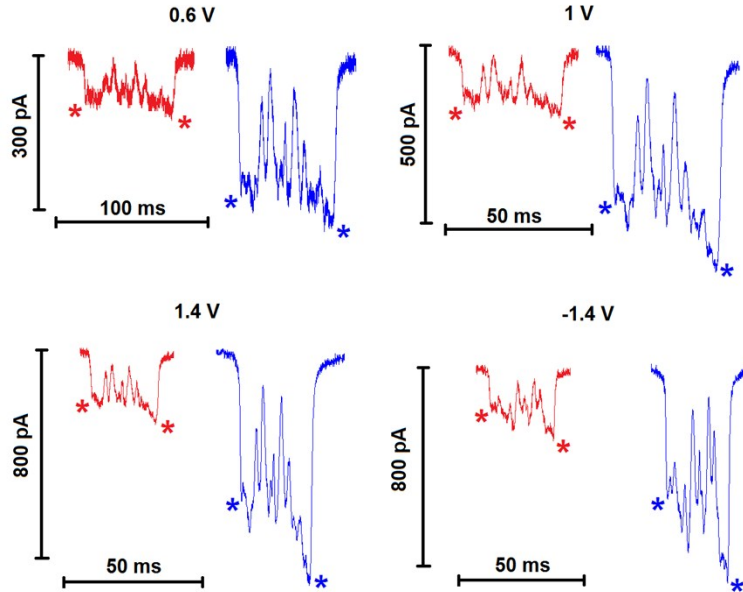


**Figure 2.** Shape of resistive pulses of 280 nm (red) and 400 nm (blue) polystyrene (PS) particles in a 660 nm in diameter PET pore under 0.1 M KCl, pH 10. (a-c) Pulses were recorded with the particle suspension being on one side of the membrane. (d) Pulses recorded when the particles were placed on the opposite side of the membrane. The asterisks (\*) denote the beginning and end peaks of the pulses used later in the analysis.

Note that in a perfectly cylindrical pore, and in the absence of pressure difference, the electroosmotic velocity features a flat profile along the radial position in the pore.<sup>1, 3</sup> Our pores, however, are characterized by finite roughness of the walls, thus the velocity is expected to have a more complex radial dependence, leading to different velocities of different streamlines the particles can follow.<sup>7, 14, 41</sup> In addition, previous reports provided estimation of the drag as a function of a ratio of the particle and pore diameters;<sup>7, 40, 42</sup> consequently, particles are expected to translocate slower if there is a tighter fit between the two sizes. Indeed, as noted above, the passage time in the 660 nm pore of 400 nm

spheres is larger than the passage time of the 280 nm beads. There is no difference in translocation velocity of 280 and 400 nm particles in the two wider pores in which the effect of walls' proximity can be neglected, as shown in Figure 3c. Note also that the larger variance of the passage time for the 280 nm beads is in agreement with the expectation that the smaller particles can probe more streamlines in the pore than the larger beads.<sup>14</sup>

41

Electroosmotic flow of solution in all cases considered here is laminar ( $Re \ll 1$ ) and we suspected the majority of particles would follow the streamlines closer to the wall, not on the pore axis.<sup>7</sup> If the particles approach the pore entrance from all directions, the probability of passage along the pore axis is indeed much lower than the off-axis transit. The preference to follow the off-axis streamlines is also evidenced by the modeling of the solution electroosmotic velocity at the pore entrance using the coupled Poisson-Nernst-Planck and Navier-Stokes equations (Figure 4).<sup>6, 16, 36</sup> Note that near the pore walls, there is a larger velocity gradient in the radial direction compared to the area closer to the pore axis. We believe that this distribution of velocity lines might also contribute to the preferential passage of the particles close to the walls. This is because the steeper gradients might lead to shorter distances over which the particles speed up; consequently, more particles will enter the pore through the off-axis paths. The wider distribution of transit times in larger pores results therefore from two effects: (i) the preference of particles to follow off-axis streamlines, and (ii) the existence of a wider spectrum of trajectories with different velocities.

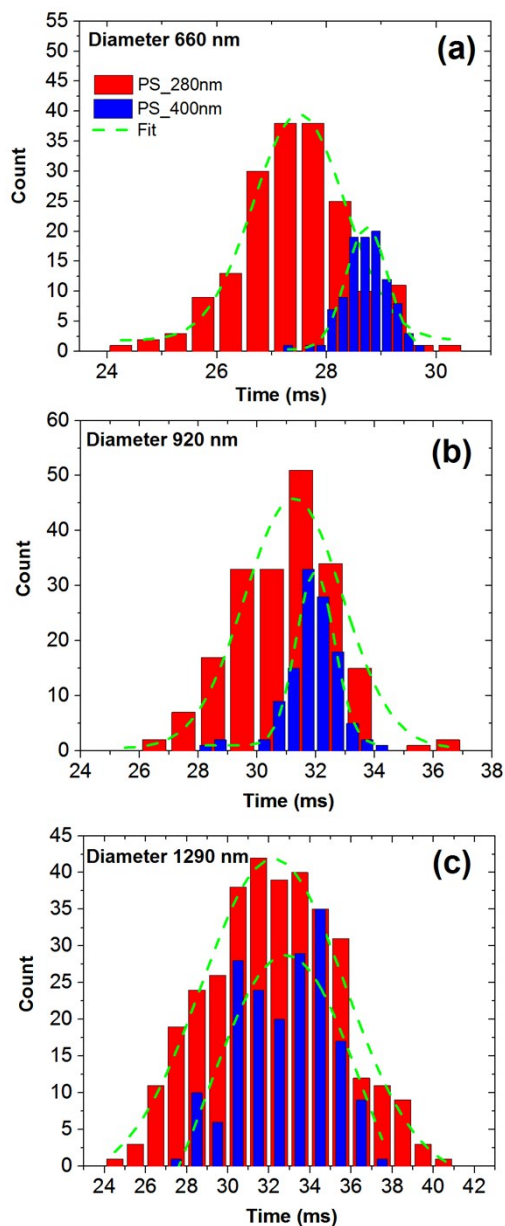


**Figure 3.** *Distribution of passage times of polystyrene particles in three independently prepared pores with different opening diameters. All data sets shown were recorded at 1.4 V. The particle suspension was prepared in 100 mM KCl, pH 10.*

*The dotted green line indicates the Gaussian fits of the distributions.*

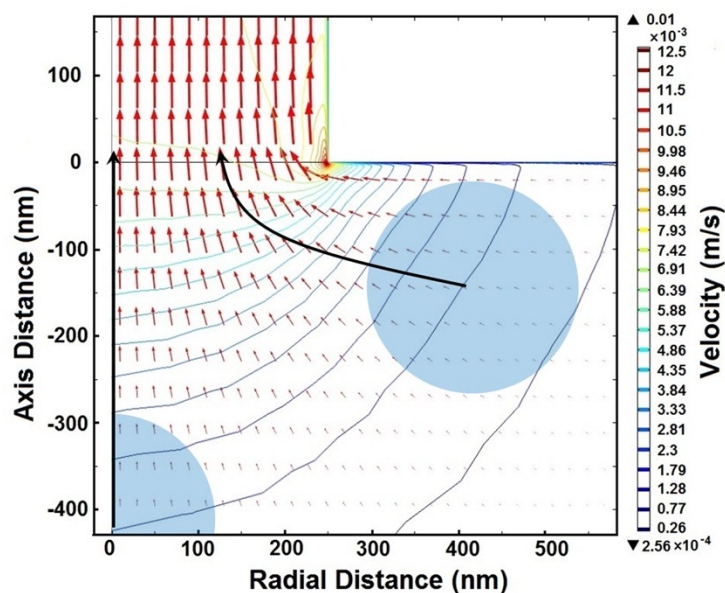


**Figure 4.** Numerical modeling of the distribution of electroosmotic velocity close to a pore entrance at 1 V in 0.1 M KCl; no particles were present in the simulations. The lines connect locations with the same velocity. In order to facilitate comparison of the distances between the lines and the particles' size, two shaded regions corresponding to the cross-section of 280 nm particles are indicated.

***Analysis of resistive-pulses corresponding to particles' passage through pores.***

In order to look for the evidence for the possible small effective surface charge on the particles, we analyzed in detail the amplitude of resistive pulses, with special attention to the beginning and end of the translocations. The edge effects associated with the surface charges of the particles and pore walls were found before to cause an increased

amplitude of the current pulse on the side in contact with a negatively biased electrode, and a decreased amplitude at the pore entrance in contact with a positively biased electrode.<sup>6, 17, 26, 29, 36, 43</sup> In meso- and micropores, the modulation of the beginning and end peaks of pulses was predicted to occur only for particles which carried finite surface charges.<sup>29</sup> The amplitude of the modulations was also reported to depend on the voltage and salt concentration in the bulk: the modulations were enhanced at higher voltages and lower salt concentrations.<sup>29, 43</sup> For a negatively charged pore, the electroosmotic flow occurs towards a negatively biased electrode,<sup>1, 3, 4</sup> so that the pulse of a particle with negative surface charges and moving in the direction of electroosmosis is expected to start with a smaller pulse amplitude. We will not consider positively charged particles, because their approach to the pore would lead to a more permanent 'sticking' of the particle to the negatively charged pore entrance, similar to results presented by Ali et al. on particle induced ionic rectifiers.<sup>44</sup>

The dependence of the pulse amplitudes in the beginning and end of the pulses on voltage and salt concentration (Figure 2) would therefore indicate presence of finite surface charges on the particle. Figure 5 summarizes results of our analysis and shows that the peaks and their ratio indeed depended on both parameters. Presence of finite surface charges of the particles was also confirmed by the zeta potential measurements; in 100 M KCl, pH 10, zeta potential of the PS particles was measured to be  $-8 \pm 1$  mV. We believe the particles can assume finite charges, e.g. due to ion adsorption.<sup>20</sup> Using the Graham equation,<sup>20</sup> and assuming that the zeta potential is close in its value to the magnitude of the surface potential, we estimated the particles' surface charge density as  $\sim -0.006$  C/m<sup>2</sup>.

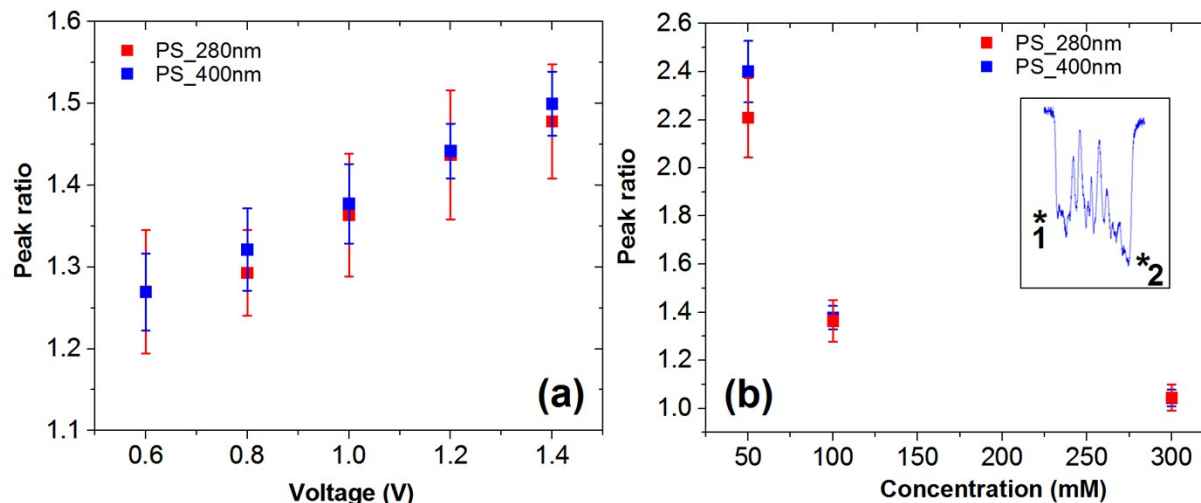


**Figure 5.** Ratios of the second and first peaks (see the inset) in the events for 280 and 400 nm PS particles in a PET pore with 660 nm in diameter at (a) different voltages, and (b) KCl concentrations in the bulk. 100mM KCl was used in (a) and 1.0 V was used in (b). The asterisks, \*, in the inset denote the beginning (end) peaks of the pulses (the peaks are marked 1, 2). The error bars indicate standard deviation of average values calculated based on at least 30 events.

In order to understand the results semi-quantitatively, we modeled resistive-pulses of particles that were neutral, as well as particles which carried low and finite densities of negative charges (Figure 6). We found that when a particle had no surface charge, the pulses had a nearly rectangular shape, with the edge currents (beginning and end of the pulses) staying voltage-independent (Figure S4). Adding  $-0.02 \text{ C/m}^2$  to the particle surface, however, changed the pulse shape, making it more asymmetric and voltage-dependent. The modeling confirmed that higher values of transmembrane potential led to a smaller current increase (larger current drop) in the beginning (end) of the pulses.

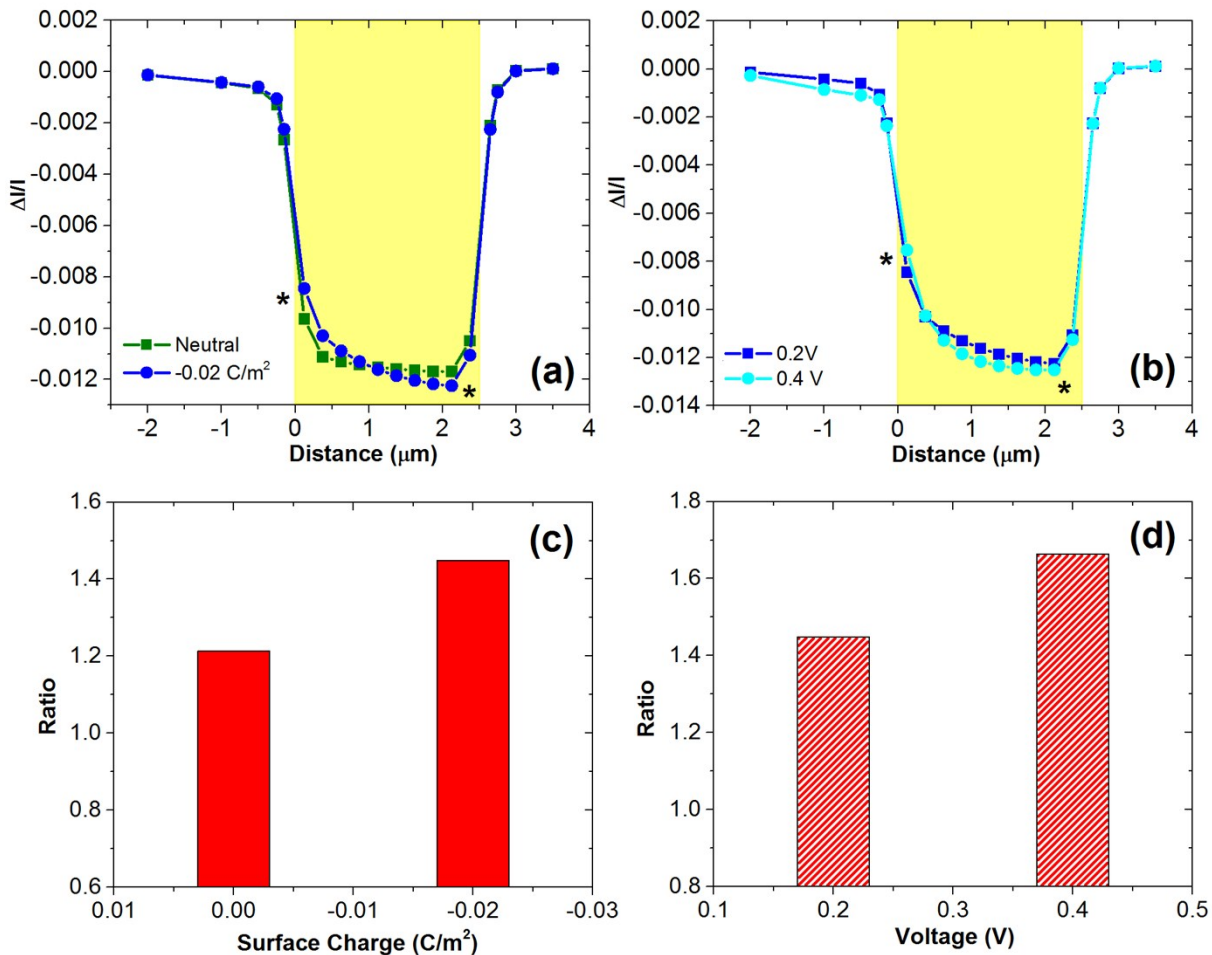


**Figure 6.** (a) Simulation of resistive-pulses of particles passing through a 500 nm in diameter and 2.5  $\mu\text{m}$  long pore in 100 mM KCl background electrolyte. The area highlighted in yellow indicates the pore interior. No surface charge as well as  $-0.02 \text{ C/m}^2$  surface charge density were considered. The asterisk (\*) symbol indicates the beginning and end peaks of the pulses. (a) Dependence of the pulse on the particles' surface charge, and (b) on the voltage for particles with  $-0.02 \text{ C/m}^2$ . (c) Ratio of ion current peaks (denoted as \* in a and b) for neutral and charged particles; (d) the same as in (c) but for two voltages and the charged particles ( $-0.02 \text{ C/m}^2$ ).

### ***Probing surface charge of particles via an approach curve.***

Examining the pulse amplitude did suggest presence of finite surface charges on the particles, but we wondered if there was another, more sensitive approach, which would allow us to test whether a particle is charged. Inspired by a method developed in the Bayley lab to probe molecules at the pore entrance without translocation,<sup>45</sup> we prepared a pore of a diameter smaller than the particles to be examined. We expected to observe a reversible blockage of the pore in the region of access resistance.<sup>46</sup> Note that this approach is different from the previous report by Ali et al.,<sup>44</sup> which discussed individual positively charged particles electrostatically attached to negatively charged pores, which resulted in ion current rectification of the pore/particle system. In our work, we assumed lack of any specific interactions between the particles and the pore walls, and we are interested in effects happening even when the particle is tens of nanometers away from the opening. An example of the ion current time signal recorded when a particle approached the pore is shown in Figure 7. The signal starts with a small current decrease, and is followed by a stable current enhancement of amplitude reaching even 10% of the baseline. Note, this biphasic character of pulses was reported before<sup>6, 26, 29, 43, 47</sup> but only for particles translocating through the pore, not approaching the entrance. The current enhancement occurred for as long as we held the voltage, which experimentally was tested up to 30 s. When recording the data, the voltage was typically held for only a few seconds for each pulse so that multiple pulses were recorded for each voltage within a relatively short time. We believe however that due to the macroscopic volume of our conductivity cell, the current enhancement would be stable over much longer time scales, perhaps even hours, since no ion depletion is expected to form.

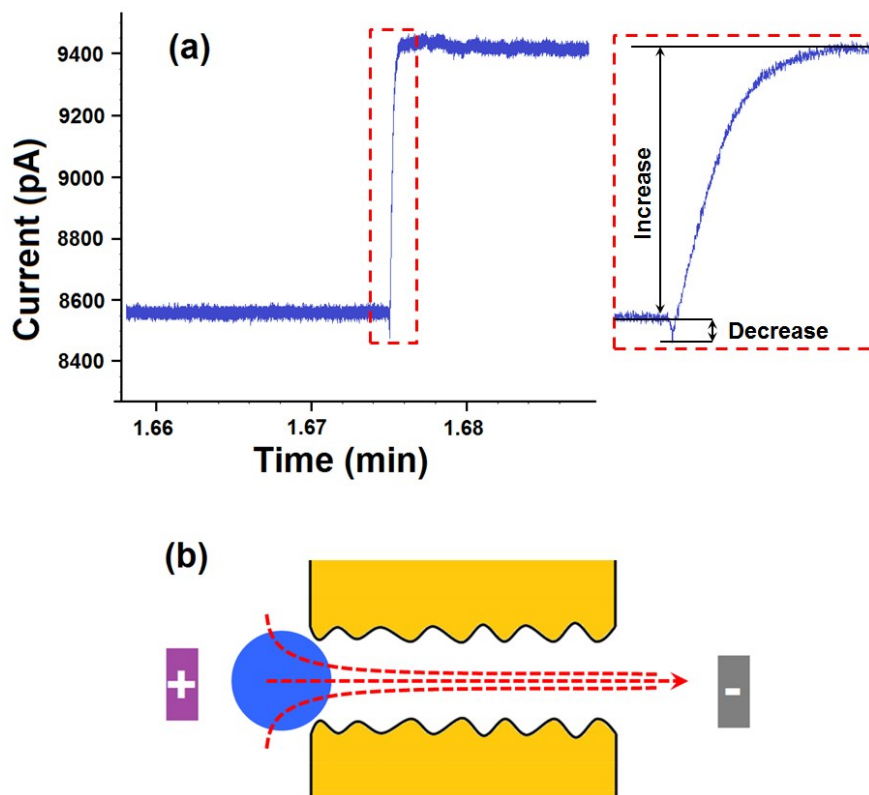


**Figure 7.** Ion current time series recorded when a 280 nm PS particle approached a 260 nm in diameter, and 11  $\mu\text{m}$  in length PET pore. A series of subsequently observed pulses, corresponding to individual particles' release and capture, is shown in Figure S5. The levels of current blockage and enhancement are stable and repeatable.

We analyzed the signal in Figure 7 and discovered that the amplitudes of both current decrease and increase were voltage-dependent (Figure 8), but surprisingly only weakly dependent on the particle size, as shown in Figure S6. Similar results were obtained using another PET pore with an opening of 380 nm in diameter (Figure S7). Note that an electrophoretic approach of negatively charged particles to the same pore, caused by

negative voltages, resulted only in current decrease (Figure 8b) that did not show any significant dependence on the particle size or particle's surface charge density either.

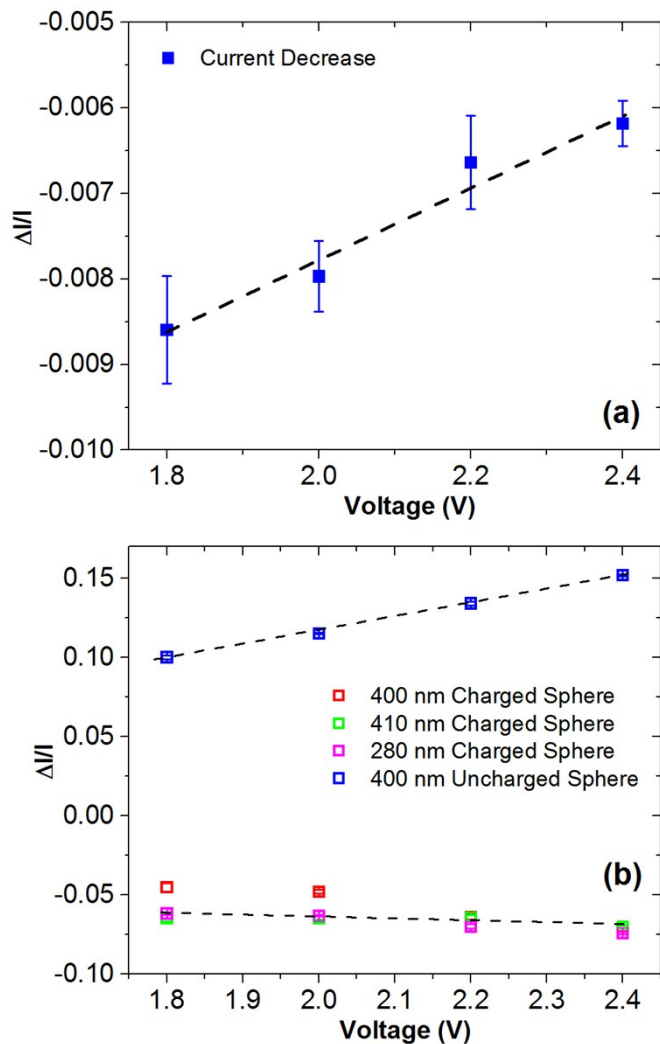


**Figure 8.** Analysis of an approach curve of the ion current signal recorded when unmodified 400 nm in diameter PS particles as well as 280, 400, and 410 nm carboxylated particles moved towards a 260 nm in diameter pore. Unmodified (carboxylated) PS particles moved in the direction of electroosmosis (electrophoresis). (a) Experimental data of a current decrease that occurred in the beginning of the approach curve of an unmodified PS particle (Figure 7). (b) Ion current change observed at the end of an approach curve for unmodified and carboxylated particles.

The error bars indicate the standard deviation of an average obtained with 5 subsequently recorded pulses for each voltage.

The qualitative interpretation of our results is as follows. The small current decrease in the biphasic pulse (Fig. 7, 8a) can be caused by a particle entering the access resistance zone.<sup>46</sup> The current increase on the other hand was postulated to report on the possible increase of ionic concentrations at the pore entrance caused by the charges on the particle, when the the particle is located within a critical distance from the pore opening. In order to support the claim, we performed numerical modeling of the transmembrane current and ionic concentrations, when the particle was located at different distances from the pore entrance (Figure 9). Note that when the center of the particle is ~150 nm away from the pore entrance, a detectable current increase above the baseline current could be expected.

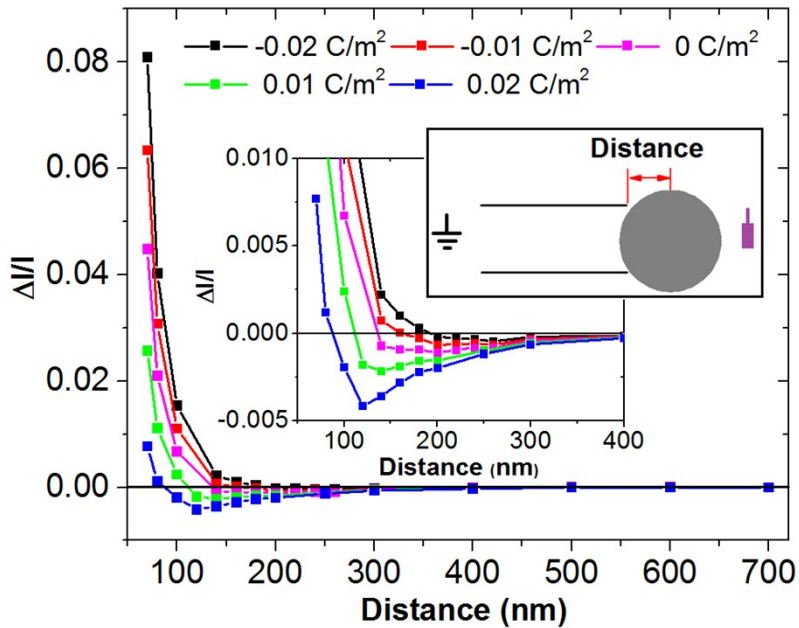


**Figure 9.** *Predicted approach curve in a form of relative change of the ion current in a particle/pore system as a function of particle distance from the pore opening and particle surface charge. The modeling was performed at 0.8 V applied across the pore. The inset shows a zoomed in region when the particle was located between 100 nm and 200 nm away from the pore opening.*

Figure 9 confirms that the biphasic character of the signal accompanying an electroosmotic approach of a particle can be reproduced by modeling, and that more negatively charged particles cause a larger current enhancement. Note that even a neutral particle is predicted to cause a current increase, however of a smaller magnitude than that of negative particles. This is in contrast to the modeling results performed for passage of neutral particles through a pore with diameter larger than the particle diameter (Figure S4), which was predicted not to cause any modulations of either of the end peaks. We also modeled the approach curve of a positively charged particle. In this case the current enhancement and the current decrease in the beginning of the pulse had similar absolute magnitudes, and did not exceed ~5% of the baseline current; note also that positively charged particles with higher charge density cause a smaller current increase. It is therefore expected that above a certain threshold of the positive charge density, only current decrease would be observed. This current decrease could be responsible for the rectifying current-voltage curves presented in the previous work by Ali et al.<sup>44</sup> Even though the modeling of the approach curve shown in Figure 9 was performed with the particle located at the pore axis, we verified that for some off-axis positions a current enhancement can be observed as well (Figure S8). As discussed below, the current

enhancement is observed when the particle diminishes the effective pore diameter below a certain threshold.

The numerical modeling of ionic concentrations in the particle/pore system helped us to further elucidate the mechanism beyond the unusual shape of the pulse accompanying an electroosmotic approach of particles to the pore opening. As mentioned above, we expected the increase of the current could be caused by modulations of local ionic concentrations at the pore entrance. Figure 10 plots average concentrations of potassium ions along the pore axis; since the pore was not ion selective the concentration of potassium and chloride was the same. We were surprised to see that presence of a particle at the pore entrance was sufficient to increase ionic concentrations in nearly half of the pore volume. An approximately 10% increase of ionic concentrations above the bulk value could therefore be responsible for the observed current increase. Figure S9 details distribution of ionic concentrations at the pore entrance.

When analyzing the experimental approach curve of a particle to a pore smaller than the particle diameter (Figure 7), we noticed it took tens of milliseconds to reach the maximum current increase. This is much longer than translocation times of the particles even in the 660 nm pore (Figure 3). The results indicate that a rather long period of time is needed to build up the increased ionic concentrations at the pore entrance and in the pore, which are responsible for the current enhancement. The tens of millisecond time scale required might explain why we do not see the increase above the baseline in the translocation experiments:<sup>6, 7</sup> the particles simply did not spend sufficient amount of time at the pore mouth to enable the enhancement of ionic concentrations to be completed.

Due to the large enhancement of ion current when a weakly charged particle approaches a pore, we proposed that measuring an approach curve could inform on small amounts of surface charge (and its polarity), which particles can acquire when in a solution. The measured signals however might not be directly informative on the magnitude of the surface charge density. The current increase accompanying the particle approach to the pore is dependent not only on the surface charge density but also the distance from the pore entrance (Figure 9). To test this claim, experiments were performed with unmodified PS and PMMA particles approaching a pore with an opening diameter of 380 nm. Both particles approached the pore by electroosmosis, but the current increase caused by the PMMA particles was higher than the current increase caused by the PS particles (Figure S10). Zeta potential of PMMA and PS particles in 0.1 M KCl, pH 10, was however measured as  $-4.5 \pm 0.5$  and  $-8 \pm 1$  mV, respectively. We hypothesize that the different magnitudes of current enhancement observed with the particles might be caused by different final positions that PMMA and PS particles assume in front of the pore entrance. It is possible that the position a particle assumes depends on the particle's surface charge and applied voltage. It is, however, difficult to distinguish whether the increase of  $\Delta I/I$  in Figure 8b with voltage is caused by a particle moving closer to the pore mouth at higher electric fields, or rather is caused by voltage modulation of ionic concentrations as discussed below.

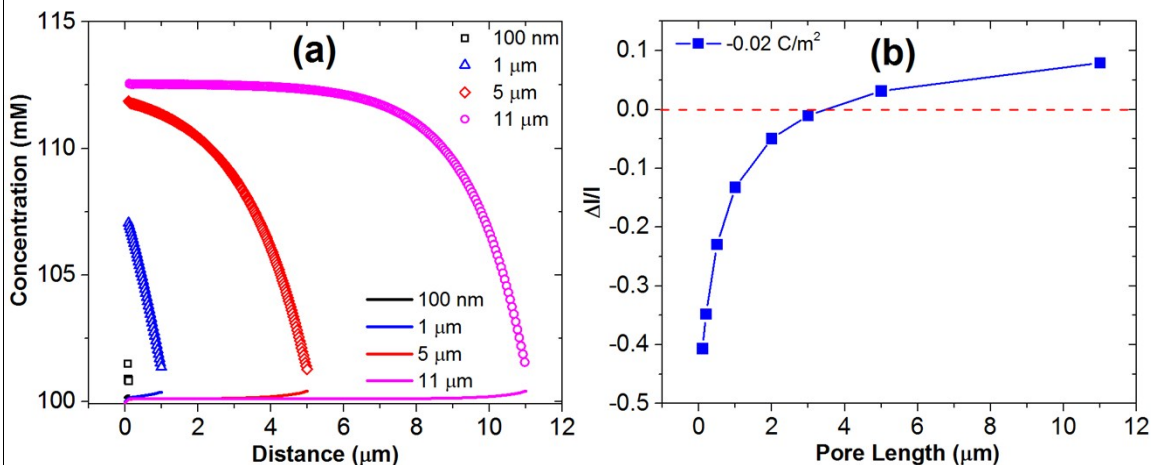


**Figure 10.** (a) Comsol simulations of distributions of  $K^+$  ions concentrations along the pore axis when a 280 nm in diameter particle was located 70 nm away from the pore opening as shown in Figure 9. **The solid lines indicate ionic concentrations of an open pore without a particle.** (b) Magnitudes of ion current through the pore with the particle present at the pore entrance as in (a). The pore had an opening diameter of 260 nm and its length was varied between 1 and 11  $\mu\text{m}$ . 0.8 V was used for the longest pore; the other voltages were selected to assure the same voltage drop across the different pore lengths.

Our experimental studies of ion current modulations accompanying a particle approach to the pore entrance is similar to the experiment in which an AFM tip was used to probe transmembrane current of a SiN film containing one nanopore.<sup>48</sup> The approach curves in the SiN system however consisted only of current decrease below the baseline current; no enhancement of ion current was seen. When we compared the two systems, SiN and our polymer pores, the main difference between them was the pore length: the SiN films were thin (<100 nm), while the length of our pores was microscopic.

Using our Comsol models, we looked therefore at the distribution of ionic concentrations in pores with various lengths (Figure 10). In all cases considered, a particle was located at the same distance from the pore opening. The results revealed that the ion current increase above the baseline value and enhancement of ionic concentrations in the pore occurred only for pores that were longer than  $\sim 4 \mu\text{m}$  (Figure 10a, b). The dependence of the current increase on the applied voltage, surface charge density of particles, and particle location is shown in Figure S11. The modeling suggested that the origin of the current increase above the baseline current could be understood by taking analogy of the particle/pore system to the conically shaped pores. When a particle is located close to the pore opening, the effective pore size indeed diminishes and is determined by the nanoconfined space between the particle and the pore walls. Applying voltage such that a positively biased electrode is placed at the narrow opening of a cone-shaped pore, leads to an enhancement of both cationic and anionic concentrations in a large fraction of the pore volume.<sup>49-52</sup> Note the ion current modulation in conical pores occurs only if the pore is sufficiently long; the threshold length depends on a few parameters including the pore diameter, opening angle, salt concentration, and voltage.<sup>53</sup> We propose that the presence of a particle at the pore mouth could be considered an analogue of a narrow opening of a conically shaped pore. In order to capture particles via electroosmosis, we place a positively biased electrode at the side of the membrane in contact with particles, thus at conditions for which enhancement of ionic concentrations is expected (Figure S12 and S13). Note that passage of unmodified PS particles through conically shaped mesopores revealed that the concentration modulations induced by voltages can indeed occur even for pores as large as 500 nm.<sup>38</sup> Numerically, we also

treated a hypothetical situation in which the particle stayed in one location, 70 nm from the pore mouth, but the voltage polarity was reversed. Note that experimentally this case could not be realized, because the induced electroosmotic flow would push the particle away. The modeling predicted that analogous to a system of conical pores, for the opposite polarity a small depletion of ionic concentrations was formed.<sup>49</sup>

Based on the experiments presented in the manuscript, we devised a system, which could be applicable to selectively pick and manipulate position of particles with low surface charge density, which are difficult to identify by other techniques. The set-up could be based on the scanning ion conductance microscope whose probe, in a form of glass pipette, could be used to capture a particle with diameter larger than the tip opening (Figure S14).<sup>54, 55</sup> We envision the pipette to be placed at the location where the particle is to be deposited; the particle's release would be induced by reversing voltage polarity. Voltage polarity during capturing process would determine whether a highly charged or nearly neutral particle was selected and moved as shown in Figure S14.

## **Conclusions**

In this manuscript we have considered electroosmotic translocations as well as an approach of particles to single pores probed as the signal of the transmembrane current. We discuss resistive-pulse experiments and point to the features of ion current pulses, which are informative on the presence of finite surface charges on the particle surface. This manuscript tackles the issue of charges on the solid/liquid interface and reminds us that any surface, even if chemically considered neutral, can acquire charges e.g. by ion

adsorption.<sup>20</sup> We show that unmodified polystyrene and PMMA particles can indeed contain small surface charge densities. The experiments with pores smaller than the particles to be detected, allowed us to trace an approach curve of individual particles moving toward the pore opening. The approach curve is the signal of transmembrane current in time that was found to consist not only of current decrease, indicative of a particle entering the access resistance, but also current enhancement when the particle moved closer to the pore opening. We identified the origin of the current increase as the enhancement of ionic concentrations in a large fraction of the pore volume. We propose using the approaches presented as a test for the existence and polarity of surface charge of particles at solid/liquid interfaces, as well as potentially to manipulate the position of individual particles.

## Acknowledgment

This research was supported by the National Science Foundation (CHE 1306058). We are grateful to the GSI Helmholtzzentrum für Schwerionenforschung for irradiation of polymers foils. We would like to thank Rachel Lucas and Cody Combs for careful reading of the manuscript.

## References

1. R. B. Schoch, J. Y. Han and P. Renaud, *Transport Phenomena in Nanofluidics*, *Rev. Mod. Phys.*, 2008, **80**(3), 839-883.
2. L. Luo, S. R. German, W.-J. Lan, D. A. Holden, T. L. Mega and H. S. White, *Resistive-Pulse Analysis of Nanoparticles*, *Annu. Rev. Anal. Chem.*, 2014, **7**(1), 513-535.
3. B. J. Kirby, *Micro-and Nanoscale Fluid Mechanics: Transport in Microfluidic Devices*, Cambridge University Press, 2010.
4. M. Firnkies, D. Pedone, J. Knezevic, M. Döblinger and U. Rant, *Electrically Facilitated Translocations of Proteins through Silicon Nitride Nanopores: Conjoint*

- and Competitive Action of Diffusion, Electrophoresis, and Electroosmosis, *Nano Lett.*, 2010, **10**(6), 2162-2167.
5. J.-P. Hsu, M.-H. Ku and C.-Y. Kao, Electrophoresis of a Spherical Particle along the Axis of a Cylindrical Pore: Effect of Electroosmotic Flow, *J. Colloid Interface Sci.*, 2004, **276**(1), 248-254.
  6. Y. Qiu, C. Yang, P. Hinkle, I. V. Vlassiouk and Z. S. Siwy, Anomalous Mobility of Highly Charged Particles in Pores, *Anal. Chem.*, 2015, **87**(16), 8517-8523.
  7. Y. Qiu, I. Vlassiouk, P. Hinkle, M. E. Toimil-Molares, A. J. Levine and Z. S. Siwy, Role of Particle Focusing in Resistive-Pulse Technique: Direction-Dependent Velocity in Micropores, *ACS Nano*, 2016, **10**(3), 3509-3517.
  8. D. T. Luong and R. Sprik, Streaming Potential and Electroosmosis Measurements to Characterize Porous Materials, *ISRN Geophysics*, 2013, **2013**496352.
  9. W. B. Coulter, U.S. Pat. No. 2,656,508, 1953.
  10. R. W. DeBlois and C. P. Bean, Counting and Sizing of Submicron Particles by the Resistive Pulse Technique, *Rev. Sci. Instrum.*, 1970, **41**(7), 909-916.
  11. R. W. DeBlois, C. P. Bean and R. K. A. Wesley, Electrokinetic Measurements with Submicron Particles and Pores by the Resistive Pulse Technique, *J. Colloid Interface Sci.*, 1977, **61**(2), 323-335.
  12. L. Berge, J. Feder and T. Jo, A Novel Method to Study Single-Particle Dynamics by the Resistive Pulse Technique, *Rev. Sci. Instrum.*, 1989, **60**(8), 2756-2763.
  13. R. R. Henriquez, T. Ito, L. Sun and R. M. Crooks, The Resurgence of Coulter Counting for Analyzing Nanoscale Objects, *Analyst*, 2004, **129**(6), 478-482.
  14. R. B. Adams and E. C. Gregg, Pulse Shapes from Particles Traversing Coulter Orifice Fields, *Phys. Med. Biol.*, 1972, **17**(6), 830.
  15. M. Tsutsui, Y. He, K. Yokota, A. Arima, S. Hongo, M. Taniguchi, T. Washio and T. Kawai, Particle Trajectory-Dependent Ionic Current Blockade in Low-Aspect-Ratio Pores, *ACS Nano*, 2016, **10**(1), 803-809.
  16. E. Weatherall, P. Hauer, R. Vogel and G. R. Willmott, Pulse Size Distributions in Tunable Resistive Pulse Sensing, *Anal. Chem.*, 2016, **88**(17), 8648-8656.
  17. A. Darvish, G. Goyal, R. Aneja, R. V. K. Sundaram, K. Lee, C. W. Ahn, K.-B. Kim, P. M. Vlahovska and M. J. Kim, Nanoparticle Mechanics: Deformation Detection via Nanopore Resistive Pulse Sensing, *Nanoscale*, 2016, **8**(30), 14420-14431.
  18. R. E. Lane, D. Korbie, W. Anderson, R. Vaidyanathan and M. Trau, Analysis of Exosome Purification Methods using a Model Liposome System and Tunable-Resistive Pulse Sensing, *Sci. Rep.*, 2015, **5**7639.
  19. W. Anderson, R. Lane, D. Korbie and M. Trau, Observations of Tunable Resistive Pulse Sensing for Exosome Analysis: Improving System Sensitivity and Stability, *Langmuir*, 2015, **31**(23), 6577-6587.
  20. J. N. Israelachvili, *Intermolecular and Surface Forces*, Academic Press, Burlington, MA, 3rd edn., 2011.
  21. D. Kozak, W. Anderson, R. Vogel, S. Chen, F. Antaw and M. Trau, Simultaneous Size and  $\zeta$ -Potential Measurements of Individual Nanoparticles in Dispersion Using Size-Tunable Pore Sensors, *ACS Nano*, 2012, **6**(8), 6990-6997.
  22. T. Ito, L. Sun and R. M. Crooks, Simultaneous Determination of the Size and Surface Charge of Individual Nanoparticles Using a Carbon Nanotube-Based Coulter Counter, *Anal. Chem.*, 2003, **75**(10), 2399-2406.

23. R. Vogel, W. Anderson, J. Eldridge, B. Glossop and G. Willmott, A Variable Pressure Method for Characterizing Nanoparticle Surface Charge Using Pore Sensors, *Anal. Chem.*, 2012, **84**(7), 3125-3131.
24. N. Arjmandi, W. Van Roy, L. Lagae and G. Borghs, Measuring the Electric Charge and Zeta Potential of Nanometer-Sized Objects Using Pyramidal-Shaped Nanopores, *Anal. Chem.*, 2012, **84**(20), 8490-8496.
25. Y. Qiu, A. Dawid and Z. S. Siwy, Experimental Investigation of Dynamic Deprotonation/Protonation of Highly Charged Particles, *J. Phys. Chem. C*, 2017, **121**(11), 6255-6263.
26. E. Weatherall and G. R. Willmott, Conductive and Biphasic Pulses in Tunable Resistive Pulse Sensing, *J. Phys. Chem. B*, 2015, **119**(16), 5328-5335.
27. R. Fan, R. Karnik, M. Yue, D. Li, A. Majumdar and P. Yang, DNA Translocation in Inorganic Nanotubes, *Nano Lett.*, 2005, **5**(9), 1633-1637.
28. Y. Zhang, G. Wu, W. Si, J. Ma, Z. Yuan, X. Xie, L. Liu, J. Sha, D. Li and Y. Chen, Ionic Current Modulation from DNA Translocation through Nanopores under High Ionic Strength and Concentration Gradients, *Nanoscale*, 2017, **9**(2), 930-939.
29. W.-J. Lan, C. Kubeil, J.-W. Xiong, A. Bund and H. S. White, Effect of Surface Charge on the Resistive Pulse Waveshape during Particle Translocation through Glass Nanopores, *J. Phys. Chem. C*, 2014, **118**(5), 2726-2734.
30. R. L. Fleischer, P. B. Price and R. M. Walker, *Nuclear Tracks in Solids: Principles and Applications*, University of California Press, Berkeley, CA, 1975.
31. R. Spohr, German Patent DE 2 951 376 C2, U.S. Patent 4 369 370, 1983.
32. P. Apel, Track Etching Technique in Membrane Technology, *Radiat. Meas.*, 2001, **34**(1-6), 559-566.
33. P. Y. Apel, Y. E. Korchev, Z. Siwy, R. Spohr and M. Yoshida, Diode-Like Single-Ion Track Membrane Prepared by Electro-stopping, *Nucl. Instr. Meth. Phys. Res. B*, 2001, **184**(3), 337-346.
34. M. Pevarnik, K. Healy, M. E. Toimil-Molares, A. Morrison, S. E. Letant and Z. S. Siwy, Polystyrene Particles Reveal Pore Substructure As They Translocate, *ACS Nano*, 2012, **6**(8), 7295-7302.
35. S. Müller, C. Schötz, O. Picht, W. Sigle, P. Kopold, M. Rauber, I. Alber, R. Neumann and M. E. Toimil-Molares, Electrochemical Synthesis of Bi<sub>1-x</sub>Sb<sub>x</sub> Nanowires with Simultaneous Control on Size, Composition, and Surface Roughness, *Cryst. Growth Des.*, 2012, **12**(2), 615-621.
36. Y. Qiu, C.-Y. Lin, P. Hinkle, T. S. Plett, C. Yang, J. V. Chacko, M. A. Digman, L.-H. Yeh, J.-P. Hsu and Z. S. Siwy, Highly Charged Particles Cause a Larger Current Blockage in Micropores Compared to Neutral Particles, *ACS Nano*, 2016, **10**(9), 8413-8422.
37. Y. Qiu, P. Hinkle, C. Yang, H. E. Bakker, M. Schiel, H. Wang, D. Melnikov, M. Gracheva, M. E. Toimil-Molares, A. Imhof and Z. S. Siwy, Pores with Longitudinal Irregularities Distinguish Objects by Shape, *ACS Nano*, 2015, **9**(4), 4390-4397.
38. Y. Qiu, I. Vlassiuk, Y. Chen and Z. S. Siwy, Direction Dependence of Resistive-Pulse Amplitude in Conically Shaped Mesopores, *Anal. Chem.*, 2016, **88**(9), 4917-4925.
39. B. Sakmann and E. Neher, *Single-channel recording*, Springer Science & Business Media, New York, 2009.

40. P. L. Paine and P. Scherr, Drag Coefficients for the Movement of Rigid Spheres through Liquid-Filled Cylindrical Pores, *Biophys. J.*, 1975, **15**(10), 1087-1091.
41. L. M. Innes, C.-H. Chen, M. Schiel, M. Pevarnik, F. Haurais, M. E. Toimil-Molares, I. Vlasiouk, L. Theogarajan and Z. S. Siwy, Velocity Profiles in Pores with Undulating Opening Diameter and Their Importance for Resistive-Pulse Experiments, *Anal. Chem.*, 2014, **86**(20), 10445-10453.
42. J. Zhu and X. Xuan, Dielectrophoretic Focusing of Particles in a Microchannel Constriction using DC-Biased AC Electric Fields, *Electrophoresis*, 2009, **30**(15), 2668-2675.
43. J. Menestrina, C. Yang, M. Schiel, I. Vlasiouk and Z. S. Siwy, Charged Particles Modulate Local Ionic Concentrations and Cause Formation of Positive Peaks in Resistive-Pulse-Based Detection, *J. Phys. Chem. C*, 2014, **118**(5), 2391-2398.
44. M. Ali, P. Ramirez, S. Nasir, Q.-H. Nguyen, W. Ensinger and S. Mafe, Current Rectification by Nanoparticle Blocking in Single Cylindrical Nanopores, *Nanoscale*, 2014, **6**(18), 10740-10745.
45. D. Rotem, L. Jayasinghe, M. Salichou and H. Bayley, Protein Detection by Nanopores Equipped with Aptamers, *J. Am. Chem. Soc.*, 2012, **134**(5), 2781-2787.
46. J. E. Hall, Access Resistance of a Small Circular Pore, *J. Gen. Physiol.*, 1975, **66**(4), 531-532.
47. E. González-Tovar, L. B. Bhuiyan, C. W. Outhwaite and M. Lozada-Cassou, Reversed Electrophoretic Mobility of a Spherical Colloid in the Modified Poisson-Boltzmann Approach, *J. Mol. Liq.*, 2016.
48. C. Hyun, R. Rollings and J. Li, Probing Access Resistance of Solid-State Nanopores with a Scanning-Probe Microscope Tip, *Small*, 2012, **8**(3), 385-392.
49. Z. S. Siwy, Ion-Current Rectification in Nanopores and Nanotubes with Broken Symmetry, *Adv. Funct. Mater.*, 2006, **16**(6), 735-746.
50. M. R. Powell, I. Vlasiouk, C. Martens and Z. S. Siwy, Nonequilibrium 1/f Noise in Rectifying Nanopores, *Phys. Rev. Lett.*, 2009, **103**(24), 248104.
51. J. Cervera, B. Schiedt and P. Ramírez, A Poisson/Nernst-Planck Model for Ionic Transport through Synthetic Conical Nanopores, *EPL*, 2005, **71**(1), 35.
52. H. S. White and A. Bund, Ion Current Rectification at Nanopores in Glass Membranes, *Langmuir*, 2008, **24**(5), 2212-2218.
53. J. F. Pietschmann, M. T. Wolfram, M. Burger, C. Trautmann, G. Nguyen, M. Pevarnik, V. Bayer and Z. Siwy, Rectification Properties of Conically Shaped Nanopores: Consequences of Miniaturization, *Phys. Chem. Chem. Phys.*, 2013, **15**(39), 16917-16926.
54. C.-C. Chen, Y. Zhou and L. A. Baker, Scanning Ion Conductance Microscopy, *Annu. Rev. Anal. Chem.*, 2012, **5**(1), 207-228.
55. P. Hansma, B. Drake, O. Marti, S. Gould and C. Prater, The Scanning Ion-Conductance Microscope, *Science*, 1989, **243**(4891), 641-643.